Title: Degradation of indole-3-acetic acid by plant-associated microbes

Lanxiang Wang [a,b,1], Yue Liu [a,c,1], Haoran Ni [a,1], Wenlong Zuo [a], Haimei Shi [a], Weixin Liao [a], Hongbin Liu [a], Yang Bai [e], Hong Yue [f], Ancheng Huang [g], Jonathan Friedman [h], Tong Si [a], Yinggao Liu[c], Mo-Xian Chen[b*], Lei Dai[a*]

[a] CAS Key Laboratory of Quantitative Engineering Biology, Shenzhen Institute of Synthetic Biology, Shenzhen Institutes of Advanced Technology, Chinese Academy of Sciences, Shenzhen 518055, China.

[b] National Key Laboratory of Green Pesticide, Key Laboratory of Green Pesticide and Agricultural Bioengineering, Ministry of Education, Center for R&D of Fine Chemicals of Guizhou University, Guiyang, 550025, China.

[c] National Key Laboratory of Wheat Improvement, College of Life Science, Shandong Agricultural University, Taian, Shandong, China.

[d] Guangdong Provincal Key Laboratory of Seed and Seedling Health Management Technology, Shenzhen Noposion Agrochemical Co., Ltd, Shenzhen, China.

[e] State Key Laboratory of Plant Genomics, Institute of Genetics and Developmental Biology, The Innovative Academy of Seed Design, Chinese Academy of Sciences, Beijing, China.

[f] State Key Laboratory of Crop Stress Biology in Arid Areas, College of Agronomy, Northwest A&F University, Yangling, Xianyang, 712100, Shaanxi, China.

[g] Key Laboratory of Molecular Design for Plant Cell Factory of Guangdong Higher Education Institutes, SUSTech-PKU Institute of Plant and Food Science, Department of Biology, School of Life Sciences, Southern University of Science and Technology, Shenzhen, Guangdong, 518055, China.

[h] Institute of Environmental Sciences, Hebrew University, Rehovot, Israel.

[1] These authors contributed equally to this work.

* Corresponding authors:

Dai Lei, CAS Key Laboratory of Quantitative Engineering Biology, Shenzhen Institute of Synthetic Biology, Shenzhen Institutes of Advanced Technology, Chinese Academy of Sciences, Shenzhen 518055, China. Email: lei.dai@siat.ac.cn

Chen Mo-Xian, National Key Laboratory of Green Pesticide, Key Laboratory of Green Pesticide and Agricultural Bioengineering, Ministry of Education, Center for R&D of Fine Chemicals of Guizhou University, Guiyang, 550025, China. Email: cmx2009920734@gmail.com

ABSTRACT

Plant-associated microbiota affect pant growth and development by regulating plant hormones homeostasis. Indole-3-acetic acid (IAA), a well-known plant hormone, can be produced by various plant-associated bacteria. However, the prevalence of microbes with the capacity to degrade IAA in the rhizosphere has not been systematically studied. In this study, we analyzed the IAA degradation capabilities of bacterial isolates from the roots of Arabidopsis and rice. Using genomics analysis and *in vitro* assays, we found that 21 out of 189 taxonomically diverse bacterial isolates possess the ability to degrade IAA. Through comparative genomics and transcriptomic assays, we identified iac-like or iad-like operon in the genomes of these IAA degraders. Additionally, the regulator of the operon was found to be highly conserved among these strains through protein structure similarity analysis. Some of the IAA degraders could utilize IAA as their sole carbon and energy source. *In planta*, most of the IAA degrading strains mitigated Arabidopsis seedling root growth inhibition (RGI) triggered by exogenous IAA. Importantly, we observed increased colonization preference of IAA degraders from soil to root according to the frequency of the biomarker genes in metagenome-assembled genomes (MAGs) collected from different habitats, suggesting that there is a close association between IAA degraders and IAA-producers. In summary, our findings further the understanding of the functional diversity and roles of plant-associated microbes.

KEYWORDS

Indole-3-acetic acid, degradation, iac-like operon, iad-like operon, MarR

INTRODUCTION

Indole-3-acetic acid (IAA) is a typical auxin naturally produced by plants, playing a crucial role in various aspects of plant growth and development, such as cell division, elongation, and differentiation [1-4]. IAA is primarily synthesized in developing plant tissues and highly concentrated in the root's apical part, where the organizing quiescent center accumulates a distinct IAA concentration gradient [5, 6]. Additionally, cells in the root apex exhibit a highly active capacity for IAA synthesis [6]. Alongside root cell exfoliation and other transportation strategies, considerable levels of IAA were detected in root exudates [7-9].

The surface and internal parts of plants are colonized by millions of commensal microorganisms, collectively known as the plant-associated microbiome [10]. Among these habitats, the root is one of the most critical, with numerous studies suggesting that root exudates, such as plant hormones, significantly influence the structure and function of the root-associated microbiome (predominantly the rhizosphere microbiome) [11-13]. Over millions of years of coexistence with their hosts, microbes have evolved multiple strategies for colonization, including the ability to synthesize and catabolize plant-specific metabolites, such as IAA [14]. It is estimated that 80% of commensal microorganisms isolated from the rhizosphere can produce IAA [15]. However, the proportion of the microbes possessing IAA degradation pathways in the rhizosphere is unknown, not to mention the potential ecological roles of these microbes in their habitats.

Two main pathways for IAA consumption among aerobic bacteria have been characterized (Supplementary Figure 1). The gene cluster *iacABCDEFGHIR*

(hereafter iac-like operon), responsible for IAA catabolism into catechol, was identified in *Pseudomonas putida* 1290, *Paraburkholderia phytofirmans* PsJN, *Acinetobacter baumannii*, *Enterobacter soli* and *Caballeronia glathei* [16-22] (Supplementary Figure 2). In contrast, the IAA degradation locus *iadABCDEFGHIJKLMNR* (hereafter iad-like operon), resulting in anthranilate as the end-product, was identified in *Variovorax paradoxus* CL14, *Achromobacter* and *Bradyrhizobium japonicum* [23-27] (Supplementary Figure 2). Moreover, among these components, heterologous expression and gene knock-out experimental validations suggested that *iacAE* or *iadDE* are necessary for IAA bio-transformation in *C. glathei* and *V. paradoxus*, respectively [22, 24]. Besides genes encoding enzymes responsible for IAA catabolism, there are components responsible for regulating operon expression in the cluster. The current studies on expression regulation of the operon suggest that most of the iac-like and iad-like operons contain a MarR (multiple antibiotic resistance regulator) family regulator [21, 24, 28]. The crystal structure of iadR and its binding properties were recently determined in *V. paradoxus*, which deciphered the operon expression regulation mechanism [24].

Here, through combining comparative genomics, transcriptomics, with *in vitro* degradation assay, we systematically evaluated the IAA degradation capacity among 189 bacterial strains which were isolated from Arabidopsis (*Arabidopsis thaliana*) and rice (*Oryza sativa*) roots. We predicted the IAA-degrading candidates based on the presence of *iacAE* and *iadDE* in their genomes, followed with experimental validation using the Salkowski method [29] combining with Liquid chromatography-mass spectrometry (LC-MS) analysis. We identified 21 strains belonging to 7 genera, including two previously unreported genera, *Sphingopyxis* and *Curvibacter*, that

typically exhibit *bona fide* IAA degradation activity. All IAA degrading strains carry the iac-like or iad-like operon, and the transcriptomic results show that iac and iad gene clusters were upregulated by IAA stimulation. Moreover, the MarR family regulator was present in the operon of all genera with high similarity in their protein structures expect for *Pseudomonas*, which had a putative two-component regulatory system in their iac-like operon. Furthermore, in subsequent assays, we found that some of the IAA degraders could utilize IAA as their sole carbon and energy source. *In planta*, our results demonstrated that exogenous IAA-induced primary root growth inhibition (RGI) was disrupted by most of the IAA degraders, suggesting an important role of IAA degraders in the rhizosphere for host plant growth and development. Finally, by analyzing metagenome-assembled genomes (MAG) and whole genome sequences (WGS) of microbial isolates from different habitats, we found that the prevalence of IAA degraders is positively correlated with naturally occurring IAA resources.

Results

Genomic analysis and experimental validation were employed to screen for IAA degraders

Previous reports have identified two types of aerobic auxin catabolic gene clusters in microbes, known as iac-like and iad-like operons [24]. Key genes *iacAE* and *iadDE* play essential roles in IAA degradation [22, 24]. To systematically evaluate IAA degradation capabilities in bacterial commensals isolated from Arabidopsis and rice root, we profiled loci containing genes homologous to *iacAE* and *iadDE* by scanning 189 bacterial genomes from our laboratory collection (Figure 1, Supplementary Table1). A total of 21 strains concurrently containing *iacA* and *iacE*, or *iadD* and *iadE*, were identified as IAA-degrading candidates. Among these, four strains belonging to

143 *Pseudomonas*, five to *Acinetobacter*, and one to *Curvibacter*, show high amino acid
144 sequence identity to the reported iacA and iacE (identity > 60%). Additionally, four
145 strains belonging to *Variovorax* and three to *Achromobacter*, exhibit high amino acid
146 sequence identity when compared to experimentally validated iadD and iadE. A strain
147 belonging to *Sphingopyxis* harbours medium amino acid identity to the iadD and iadE
148 (identity between 40% to 60%). Interestingly, the genomes of three *Sphingomonas*
149 strains contain both iacAE and iadDE with medium amino acid identity (Figure 1),
150 (Supplementary Table2).
151
152 To validate the predicted results, we tested the IAA degradation capability among the
153 137 Arabidopsis root bacterial isolates and 6 IAA-degrading candidates from rice
154 collections by using the Salkowski reaction method. After 72' hours incubation,
155 bacterial growth and the percentage of IAA degradation of the strains were measured
156 and calculated. A total of 32 out of 143 strains displayed considerable IAA
157 degradation efficiency, such that over 30% of the IAA content were consumed
158 (Supplementary Figure 3A). Among them, 21 IAA-degrading candidates possessing
159 iacAE or iadDE, consumed over 50% of the IAA content in the medium after 72- hour
160 incubation (Supplementary Figure3B). To further detect the consumption of IAA by
161 the IAA-degrading candidates, the supernatant of the culture was analyzed by a
162 highly accurate analytical approach of LC-MS. The specific peak of the IAA was
163 undetectable in these IAA-degrading candidates cultures, suggesting that IAA was
164 degraded by these strains (Supplementary Figure 3C). Ultimately, 21 IAA degraders
165 belonging to seven genera were confirmed through experimental validation, which
166 are consistent with the bioinformatics prediction.
167

IAA degraders possess the iac/iad-like operon

To clarify and characterize the IAA catabolism gene clusters in our screened IAA degraders, we performed a BLASTp search using the amino acid sequences of the full iac and iad operons obtained from previous reports against the genomes of 21 strains (Supplementary Figure 2, Supplementary Table 2). A complete iac-like or iad-like operon was identified from the genome of all the IAA degraders except for *Sphingopyxis*_Root154 (Figure 2A). Consistent with previous reports, strains from *Achromobacter* and *Variovorax* possess the iad-like operon, and strains from *Pseudomonas*, *Acinetobacter* and *Sphingomonas* contain the iac-like operon in their genomes. For *Curvibacter*_SE9, and *Sphingopyxis*_Root154, two novel identified IAA-degrading genera, a iac-like operon and a fragmented iad-like operon are present in their genomes, respectively (Figure 2A). Additionally, aside from the complete iac-like operon, two sets of fragmentary iad-like gene clusters were also found in the genomes of strains from *Sphingomonas* (Supplementary Figure 4). Intriguingly, there is another potential fragmented iad-like operon (iad-2) present in the genome of *Sphingopyxis*_Root154, and this operon has the same gene cluster arrangement with strains from *Spingomonas* (Supplementary Figure 4).

To investigate the evolutionary relationships among different IAA degraders, we constructed a phylogenetic tree using concatenated iacAE or iadDE amino acid sequences. Intriguingly, strain organization in this tree differed substantially from the phylogenetic relationships based on 16S rRNA sequences (Supplementary Figure 5). *Curvibacter* was more closely related to *Acinetobacter* than to other Burkholderiales. *Sphingomonas* and *Sphingopyxis*, both belonging to Sphingomonadales, appeared on different branches. Moreover, *Sphingomonas* genomes contained iac-like operon,

193 while the *Sphingopyxis* genome harbored an iad-like operon (Figure 2A). These
194 results suggest that, evolution of microbes un-synchronized with some gene cluster
195 acquisition.
196
197 **The MarR family regulators exhibit high degree of structural conservation**
198 **among IAA-degrading strains**
199 In all IAA-degraders except *Pseudomonas*, both iac-like and iad-like operons contain
200 one or two MarR-family regulator (R) that are involved in the operon expression
201 regulation (Figure 2A). In contrast to previous reports [24], our four *Pseudomonas*
202 strains exhibited the involvement of a putative two-component regulatory system in
203 their iac-like operons (Figure 2A) . Upon comparison with the iac operon in the related
204 reference strain *Pseudomonas putida* 1290, it seems that the components of the
205 cluster may have been acquired from a distant genus, such as *Paraburkholderia*
206 *phytofirmans* (Supplementary Figure 2).
207
208 Generally, the MarR regulator acts as a negative transcriptional factor for the operon
209 since it binds to the upstream DNA region, inhibiting operon expression. Due to the
210 similar role of this protein in regulating iac and iad operon expression, we
211 hypothesized that they are homologous with high amino acid sequence identity. To
212 verify our hypothesis, multiple protein sequence alignment was performed using 21
213 potential MarRs identified from our 17 strains and six MarR reference proteins [24].
214 Consistent with previous reports, MarR regulators are diverse, as they have low
215 protein sequence identity (Supplementary Figure 6). The phylogenetic tree based on
216 the protein sequence of 27 MarRs demonstrated that iacR naturally separated from
217 iadR (Figure 2B), which is consistent with previous reports [30]. MarRs are relatively

conserved within a genus, while iacRs display more sequence diversity. It is worth noting that three strains from *Sphingomonas* contain two iacRs in their iac operons, respectively (Figure 2 and Supplementary Figure 6). Also, two MarRs were screened from Root154_*Spingopyxis* genome with low similarity, Root154_1 (gene_00256) and Root154_2 (gene_00334) (Figure 2B, Supplementary Figure 6). In addition, except for Root154_1 (gene_00256), other MarRs from Sphingomonadaceae were grouped together and classified as iacR (Figure 2B).

To further elucidate the mechanism of functional conservation among MarRs, the predicted protein structures of 21 hypothetical MarRs were generated using AlphaFold2 [31] (Supplementary Figure 7). The protein structures of six referential MarRs were retrieved from the PDB, and pairwise comparisons were performed among the 27 MarRs using TM-align [32]. As shown in the heatmap, all pairwise comparisons obtained a high TM score (all pairwise TM score > 0.5) [33] (Figure 2B), suggesting that all MarRs displayed high similarity in their protein structures. In addition, the IAA binding sites of MarRs also exhibited high conservation, especially within a genus level (Figure 2B).

Iac- and iad-like operons were up-regulated by IAA

To explore how iac- or iad-like operons were regulated by IAA, we examined the transcriptomes of five strains in response to this compound. The strains selected for RNA-seq were *Pseudomonas*_Root71, *Achromobacter*_Root170, *Variovorax*_Root473, *Curvibacter*_SE9, and *Sphingopyxis*_Root154. They were cultured with M9 minimal medium supplemented with IAA or glucose, and cells were collected in specific time point (see method). Among them, *Curvibacter* and

Sphingopyxis were studied for IAA degradation activity for the first time. In total, 308, 151, 274, 871, and 220 differentially expressed genes (DEGs) were identified in these five strains, respectively (Supplementary Table 3). Both iac-like and iad-like operon were significantly upregulated by IAA, except for Root154 (Figure 3). Furthermore, categorization of up- and down-regulated DEGs indicated that IAA treatment broadly influenced many metabolism pathways (Supplementary Figure 8).

It has been reported that chemicals in root exudates may enhance plant-microbe interactions through transcriptional regulation of bacterial motility [34]. Flagella are organelles used by microbes for movement. Notably, in Root473 and Root154, genes involved in flagellar biosynthesis, and chemotaxis proteins were upregulated by IAA treatment when compared with glucose control, suggesting that for these two strains, IAA might be more attractive than glucose. However, in SE9, genes encoding flagellum-related DEGs and chemotaxis proteins were down-regulated by IAA stimulation, indicating that IAA elicited different molecular responses in different strains. Consistent with previous reports, catechol, the end-product of iac-pathway , will be further catalyzed by downstream enzymes, catABC [16, 20, 21]. Genes involved in catechol pathway in Root71 and Root170 were up-regulated by IAA treatment (Supplementary Table 3, highlighted).

IAA can be utilized as the carbon source

To evaluate the utilization of IAA by the IAA degraders, *in vitro* assay were preformed among the screened 21 IAA degraders. The IAA degradation efficiency and bacterial growth of the strains were carried out in M9 minimal medium with exogenous IAA. Results showed that except for strains from *Sphingomonas* and *Sphingopyxis*, other

strains benefited from IAA as the sole carbon source and completely consumed IAA within 72 hours (Figure 4A). Strains from *Acinetobacter* presented the maximum degradation and growth rates, consuming IAA completely within 12 hours (Figure 4A and B). Compared with strains from *Acinetobacter*, strains from *Pseudomonas* displayed the equivalent IAA degradation efficiency and less biomass. Strains from *Variovorax*, *Achromobacter*, and *Curvibacter*, which generally degraded IAA completely within 60 hours, also showed extremely slow growth rate may suggest that cell proliferation of these strains require more carbon and energy source. On the other hand, strains from *Sphingomonas* only consumed partial IAA in the M9 minimal medium, while *Sphingopyxis* barely utilized this compound under this condition of culture. Combined with the transcriptome analysis, our results here suggest that IAA triggered the expression of iac/iad operon and biotransformed this compound in the medium, although the by-products of IAA degradation may not suitable for cell growth as sole carbon and energy source.

IAA degraders contribute to the regulation of plant root growth

Auxin homeostasis in plant roots is achieved through local synthesis, polar transport, and the contribution of IAA-producing/consuming microorganisms, which is crucial for root growth. To clarify the biological role of the root isolates possessing IAA degradation capability identified in this study, seven-day-old Arabidopsis seedlings were transferred to 1/2 MS agar medium supplemented with 100nM IAA and inoculated with the IAA degraders individually. After additional seven days of inoculation, primary root elongation was measured. Primary root elongation was suppressed when exogenous IAA was added to the medium (Figure 4C and E). In mono-associations, normal primary root growth was observed when seedlings were

293 inoculated with strains from *Pseudomonas*, *Variovorax*, *Achromobacter*,
294 *Sphingomonas*, *Curvibacter*, and SB9, the only strain from *Acinetobacter* (hereafter
295 referred to as RGI-suppressive IAA degraders, while the rest are
296 RGI-non-suppressive IAA degraders) (Figure 4C and E, Supplementary Figure 9).
297 Consistently, a small range of fresh weight enhancement of shoots was observed in
298 these positive mono-associations (Figure 4D). On the other hand, the rest strains
299 from *Acinetobacter* inhibited primary root elongation, as well as shoot fresh weight
300 (Figure 4C and D). No significant effects on root growth or shoot fresh weight were
301 observed in *Sphingopyxis* treatment.
302
303 To further explore whether the restoration of RGI by RGI-suppressive IAA degraders
304 is directly related to auxin signaling in plants, the Arabidopsis auxin reporter line
305 *DR5::GFP* was treated with IAA and simultaneously inoculated with IAA degraders.
306 Fluorescence of the *DR5::GFP* induced by exogenous IAA remained stable in axenic
307 control at day 1 and day 3 post-inoculation. The GFP signal in *DR5::GFP* roots was
308 quenched at day 3 after inoculation with RGI-suppressive IAA degraders. Consistent
309 with the root elongation phenotype, RGI-non-suppressive IAA degraders, including
310 strains from *Sphingopyxis* and *Acinetobacter*, could not quench the root fluorescence
311 caused by exogenous IAA (Figure 4E, Supplementary Figure 9). Interestingly, SB9,
312 the RGI-suppressive IAA degrader from *Acinetobacter*, quenched the fluorescence at
313 day 3 (Supplementary Figure 9). To rule out the possibility that the phenomenon
314 observed in RGI-non-suppressive IAA degraders was not caused by failed
315 colonization, colonization of strains was investigated by calculating colony-forming
316 units (CFUs), which were further normalized to root fresh weight. After seven days of
317 inoculation, all strains successfully colonized roots, and exogenous IAA

supplementation had no significant effect on bacterial colonization (Supplementary Figure 10 and 11).

Catalogue of potential IAA-degrading bacteria from diverse habitats

IAA degrading bacteria in the rhizosphere play an important role in maintaining auxin homeostasis in roots to ensure normal plant growth and development [25]. Nevertheless, their distribution across various habitats remains limited. To ascertain the distribution of IAA-degrading strains in different habitats, we analyzed a large-scale survey of 11,586 high-quality MAGs (including 750 isolates) collected from mammal gut, aquatic environment, soil and plants (Figure 5) (Supplementary Table 4) [35-43]. The iacA/E and iadD/E were used as the biomarkers to screen the genomes of the collections. We noted that no hits were identified in MAGs collected from cold seeps or animal/human guts, which are reasonable since these habitats are normally hypoxic, while the iac/iad pathways are aerobic (Supplementary Table 4) . Furthermore, iac or iad-like operon is also absent in the facultative anaerobic environment of the human oral [43]. In contrast, among the 692 MAGs collected from human skin, five potential IAA degraders containing iac-like operon were identified [43].

On the other hand, more potential IAA degraders were identified from environment samples, especially plant-associated samples. 0.65% MAGs (2 out of 304) collected from marine samples [43], and 1.63% MAGs (8 out of 492) collected from wastewater samples were identified harboring iad-like operon [42]. In soil samples, 1.31% MAGs (5 out of 382) were identified containing iac or iad-like operon [35, 42]. Within the plant collections, 3.79% MAGs (5 out of 132) affiliated with Sphingomonadales and Burkholderiaceae were identified as containing the iac or iad-like operon [42].

Furthermore, 7.60% MAGs (60 out of 789, containing 206 isolates) collected from plant shoot [36, 38, 40] and 12.13% MAGs (66 out of 544, all are isolates) isolated from plant root [40, 41] were found to harbor the IAA degradation operon. Overall, there is a consistent increase in the frequency of potential IAA degraders from aquatic to terrestrial environments, from soil to plants, and from plant shoots to roots. Moreover, potential IAA degraders containing iac- or iad-like operon and belonging to Burkholderiales were widely distributed across various habitats (Figure 5).

DISCUSSION

In this study, combining genomic analysis and experimental validation, we performed a systematic screening of IAA degraders isolated from Arabidopsis and rice root. We found that 21 strains belonging to 7 genera exhibit remarkable IAA degradation activity. In addition to the previously reported *Pseudomonas*, *Achromobacter*, *Variovorax*, *Acinetobacter*, and *Sphingomonas*, strains from *Sphingopyxis* and *Curvibacter* also displayed outstanding IAA-degrading activity. The genomes of all IAA degraders contain iac- or iad- like IAA degradation operon, and these operons were upregulated by IAA treatment. By integrating protein sequence alignment with protein structural similarity analysis, we revealed that the MarR family regulators are structurally conserved within genus. *In vitro* assays suggested that the screened 21 strains are *bona fide* IAA degraders. However, only a subset of these strains directly depleted exogenous IAA to maintain the host-plant root growth. Intriguingly, MAGs analysis showed that IAA-degrading candidates naturally colonized plant-associated habitats, which aligns with the notion that IAA degraders are prevalent in habitats closely linked to IAA producers. Our findings revealed a key role of IAA degraders inhabiting in plant and the underlying degradation mechanism.

Comparative genomics studies indicate that the gene clusters of IAA degraders were probably acquired in a natural environment through a horizontal gene transfer pathway, with selective loss, duplication, and rearrangement of IAA-degrading genes during evolution. The gene cluster contains structural genes encoding enzymes responsible for IAA degradation and a set of genes involved in gene expression regulation and compound transportation, and the core components are highly conserved. The structure and arrangement of the iad-like operon in *Variovorax* are highly similar to that in *Achromobacter*, indicating that these two genera belonging to Burkholderiales may have obtained the operon from the same ancestor/donor. In contrast, *Curvibacter*, another genus belonging to Burkholderiales, possesses the iac-like operon, suggesting the possibility that IAA degradation gene clusters were obtained through horizontal gene transfer (Supplementary Figure 5). *Sphingomonas* and *Sphingopyxis* are closely related and both belong to the Sphingomonadaceae. A complete iac-like operon uniquely present in the genomes of strains from *Sphingomonas*. Moreover, IAA-degrading gene cluster mining analysis showed that two additionally fragmentary iad-like operons exist on *Sphingomonas* genomes, and one of them has the same gene arrangement to the *Sphingopyxis* (Supplementary Figure 4), suggesting the evolutionary homology of these two genera. Additionally, although *Acinetobacter* and *Curvibacter* belong to different families, both genera have iac-like operons and the operons have the similar gene arrangement, suggesting that they may obtained the gene cluster from a closer donor (Figure 2A).

IacR and iadR are an essential component of the IAA-degrading gene cluster, and functional studies suggest that it normally serves as an expression suppressor of the

operon. Recently, the protein crystal structure of iadR was resolved, and it was confirmed that iadR binds to the upstream DNA sequence of *iadA* to inhibit iad locus expression in *Variovorax paradoxus* CL14 [24]. The presence of IAA results in iadR being released from the DNA binding site, further disinhibits the expression of the iad operon. The MarR regulators have highly conserved protein structures despite having highly differentiated protein sequences (Supplementary Figure 6 and 7, Figure 2B). This may explain why different MarR regulators perform similar functions in regulating operon expression. Similar to *Paraburkholderia phytofirmans* PsJN, LuxR and iacS uniquely exist in the iac operons of four strains belonging to *Pseudomonas*, suggested that a putative two-component regulatory system independently evolved or obtained in this genus (Figure 2A) [20].

Plant growth requires multifaceted regulation, including but not limited to IAA production and degradation by plant, as well as auxin regulation by plant-associated microbiota [25]. It is estimated that 80% of rhizosphere commensal isolates possess the capability of producing IAA [15]. While, based on our results, only 11.11% of the isolates (21 out of 189 in this study) and 7.84% (131 out of 1465) of the plant-associated MAGs (Supplementary Table 4) exhibit potential IAA-degrading capability. The results of mono-association further reveal the biological role of IAA degraders in manipulating IAA homeostasis in plants to maintain root growth. However, not all IAA-degrading strains have the ability to reverse the severe inhibition of root growth induced by excess IAA. Moreover, our mono-association results showed that *Acinetobacter* has negative effects on plant growth (Figure 4, Supplementary Figure 9), which is inconsistent with recent reports that *Acinetobacter* can act as a plant growth-promoting rhizobacteria (PGPR) [44, 45]. In addition to

418 being a strong IAA-degrading bacterium, *Acinetobacter* is also one of many that
419 produce IAA and can thus sabotage plant physiology by adding to the endogenous
420 IAA pool in plants [46]. Given these contradictory traits, the biological function of
421 *Acinetobacter* for plants and the underlying mechanism need to be further studied.
422
423 Our large-scale MAGs analysis results suggested that the prevalence of
424 IAA-degrading taxonomy increased gradually from aquatic to terrestrial environments,
425 from soil to plants, and from plant shoots to roots (Figure 5). It is reasonable that
426 IAA-degrading bacteria may be recruited to utilize IAA as sources of carbon and/or
427 nitrogen, whereas plants and numerous plant-associated IAA-producing microbes
428 serve as natural sources of this compound.
429
430 Lastly, hormones may play a crucial role in mediating the interactions between hosts
431 and microbes. For instance, *Mycobacterium neoaurum* possessing the capability to
432 degrade testosterone was isolated from the fecal samples of testosterone-deficient
433 patients with impression. Further experiments revealed the potential association
434 between human gut microbes expressing 3β-HSD and depressive symptoms
435 resulting from testosterone degradation [47]. Beyond IAA, other plant hormones have
436 been reported to be synthesized or metabolized by microbes. For examples,
437 rhizobacteria such as *Rhodococcus* sp. P1Y and *Novosphingobium* sp. P6W have
438 been reported to utilize abscisic acid (ABA), consequently stimulating plant growth
439 through an ABA-dependent mechanism [48]. We envision that investigations on
440 microbial metabolism of host hormones may offer novel insights into the
441 understanding of homeostasis, host physiology and the development of diseases.
442

MATERIALS AND METHODS

Plant materials and bacterial strains

Arabidopsis thaliana ecotype Columbia (Col-0) was obtained from laboratory stock. The Arabidopsis auxin reporter transgenic line *DR5::GFP* was kindly provided by Prof. Xugang Li (Shandong Agriculture University). The 137 bacterial commensals isolated from Arabidopsis roots or soil were gifts from Prof. Paul Schulze-Lefert (Max Planck Institute for Plant Breeding Research, Cologne, Germany)[40]. Detailed information on individual strains can be found at At-RSPHERE (http://www.at-sphere.com/).

The 52 rice root-associated bacterial isolates analyzed in this study were retrieved from our laboratory stock. In detail, rice root samples contain bulk soil were collected in field and immediately delivered with ice to our lab. After removed the bulk soil, 10g root samples contain rhizosphere soil were washed multiple times with sterilized water until there is no obvious soil on root surface. The washings were mixed as the rhizosphere sample. Rice roots were then grind with 10ml 1 × PBS buffer in a sterilized mortar and filtered with sterilized gauze. Both samples were then spread on the surface of 1/5TSB agar plates with series dilution. After incubation for 3 days at 25℃, single colonies were randomly picked from the plates for twice purification. A total of 207 isolates were identified at the species level by sequencing 16S rRNA gene with the primers 27F (AGAGTTTGATCCTGGCTCAG) and 1492R (GGTTACCTTGTTACGACTT). For whole genome sequencing, the genome DNA of selected 72 strains were individually extracted using FastDNA Spin Kit for Soil (MP Biomedicals, USA). Library preparation was performed using the Hieff NGS OnePot II DNA Library Prep Kit (Yeasen, China) for Illumina with 50 ng DNA per sample. The

468 draft genomes were generated with the HiSeq Xten platform (Illumine, USA). Quality
469 control of the raw reads were filtered with fastp [49], followed with genome assembly
470 through Unicycler[50]. CheckM was used to estimate the quality of each genome,
471 including the numbers and N50 of the contigs, the contamination, and the
472 completeness[51]. Prokka was used to annotate the function of all assembled
473 genomes[52]. Taxonomy annotation of the isolates was performed using the Genome
474 Taxonomy Database Toolkit (GTDB-Tk)[53] with reference to GTDB release 207[54].
475 Isolates were assigned at the species level if the ANI to the closest GTDB-Tk
476 representative genome was ≥95% and the aligned fraction was ≥60%. General
477 taxonomical information of these 189 strains is listed in Supplementary Table 1.
478

479 **Construction and modification of phylogenetic tree**

480 The phylogenetic trees were constructed using MUSCLE[55] for multiple sequence
481 alignment and MEGA[56] for tree construction. Specifically, Figure 1 was constructed
482 using the 16S rRNA from 189 strains; Figure 2A was constructed using the amino
483 acid sequences of key genes involved in IAA metabolism from 21 IAA-degraders;
484 Figure 2B was constructed using the amino acid sequences of 21 MarR proteins
485 discovered from the 17 IAA-degraders and 6 related templates. The generated
486 phylogenetic trees were further visually modified using iTOL[57].
487

488 **Identification of potential IAA-degraders**

489 Prokka[52] was used for functional annotation of isolates and MAGs derived from
490 different environments, meeting the criteria of genome completeness (≥90%) and
491 contamination (≤5%). Diamond[58] was employed for sequence alignment of
492 annotated genomes, using previously reported IacA and IacE or IadD and IadE

493 sequences as templates. The alignment filtering threshold was set at sequence
494 similarity (Identity) >50% and sequence coverage (Coverage) >60%. If both gene
495 combinations were simultaneously identified in a genome and determined to be
496 located in the same gene cluster (IadD adjacent to IadE; IacA with a distance less
497 than 7 Coding Sequences (CDS) from IacE), the strain was considered to possess
498 IAA degradation capability.
499
500 **Bacterial culture and screening of IAA degradation**
501 Individual bacteria from glycerol stock were incubated on 1/2 tryptic soy broth (TSB,
502 Sigma-Aldrich, USA) agar plates at 25°C for 5 days. A single colony of each strain
503 was then cultured in 1/2 TSB liquid medium at 25°C with 400 rpm shaking. When the
504 cell culture reached the exponential growth phase, the optical density of the culture
505 was measured at 600 nm (OD_{600}) using a SynergyTM H1 microplate reader (BioTek,
506 USA).
507
508 The bacterial culture was washed once with 1×PBS and then added to 1 mL of 1/2
509 TSB medium supplemented with or without 0.4 mM IAA (Sigma-Aldrich, USA) to
510 achieve a final OD_{600} of 0.05. After 72 hours of incubation at 25°C with 400 rpm
511 shaking, the IAA content of each sample was measured using the Salkowski method
512 [29]. Briefly, 120 µL of Salkowski reagent was mixed with 60 µL supernatant of culture,
513 and the absorbance of the mixture was measured at 530 nm after 30 minutes of
514 incubation in the dark. The remaining IAA contents in the medium were then
515 calculated using IAA standard curves. The bacterial degradation rate was further
516 calculated as the IAA consumed divided by the initial IAA content in the culture.
517

518 **Validation of IAA degradation by LC-MS analysis**

519 To validate the IAA degradation results of the Salkowski method, cell cultures of
520 selected strains were further analyzed by LC-MS [29]. After 72 hours of incubation
521 with IAA, the cell cultures were collected to test the content of IAA in the medium. In
522 detail, the residual IAA of the cell cultures was extracted twice with ethyl acetate,
523 followed by volatilization, and the residue was further dissolved in 80% methanol.
524 After filtration, a 2 μL sample was separated using a C18 column (Infinity Lab
525 Poroshell 120 EC-C18, 2.1 × 50 mm, 2.7 μm; Agilent, USA) connected to the Agilent
526 6470B triple quadrupole LC/MS (Agilent, USA). Solvent A (water supplemented with
527 0.1% formic acid) and solvent B (acetonitrile supplemented with 0.1% formic acid)
528 were used as mobile phases at a flow rate of 0.2 mL/min under a gradient elution: 0-2
529 min, 10% B; 2-8 min, 40% B; 8-11 min, 70% B; 11-15 min, 10% B. The quantification
530 of IAA extracted from culture and IAA standards was performed using the positive-ion
531 multiple reaction monitoring (MRM) method.

532

533 **Growth experiment with IAA as the sole carbon source**

534 Selected IAA degraders were individually cultured at 25°C with 400 rpm shaking in 1
535 mL M9 minimal salts medium (Sigma-Aldrich, USA), supplemented with 2 mM $MgSO_4$
536 and 0.1 mM $CaCl_2$. A 0.4 mM IAA solution was added to the culture as the sole
537 carbon source. OD_{600} and IAA concentrations were measured at 7 time points: 0 h, 12
538 h, 24 h, 36 h, 48h, 60 h and 72h.

539

540 **RNA-seq and data analysis**

541 *Pseudomonas*_Root71, *Achromobacter*_Root170, *Variovorax*_Root473,
542 *Curvibacter*_SE9, and *Sphingopyxis*_Root154 were grown in 1 mL M9 medium

543 supplemented with 1.712 mM glucose or 1 mM IAA. The initial OD_{600} of the cultures
544 was 0.05, and they were incubated at 25°C with 400 rpm shaking. Cells from
545 *Pseudomonas*_Root71, *Achromobacter*_Root170, *Variovorax*_Root473,
546 *Curvibacter*_SE9, and *Sphingopyxis*_Root154 were collected for RNA-seq at 14 h, 16
547 h, 14 h, 48 h, and 20 h, respectively. Bacterial pellets were collected by centrifuging
548 the culture at 12,000 rpm for 10 min at 4°C. The pellets were stored at -80°C until
549 RNA extraction.
550
551 Further experiments including RNA extraction, library preparation and sequencing
552 were preformed at Magigene Co. Ltd using the Nova Seq6000 platform (Illumine,
553 USA). In detail, bacterial RNA samples were extracted using the Trizol followed with
554 quality control by Thermo NanoDrop One and Agilent 4200 Tape Station. Epicentre
555 Ribo-Zero rRNA Removal Kit was using to remove Ribosome RNA in the samples.
556 Library preparation was performed using the NEBNext Ultra Directional RNA Library
557 Prep Kit for Illumina (New England Biolabs; USA) with 1 μg total RNA per sample.
558 The raw data were processed with RNA-seq pipeline from nf-core (nf-core/rnaseq,
559 v3.11.1) [59], with trimming enabled. The clean reads were then mapped to the
560 reference genome of corresponding strain with STAR (v2.7.10a) [60]. Gene
561 quantification was subsequently done using Salmon (v1.5.2) [61]. Differentially
562 expressed genes (DEGs) were identified using DESeq2 (v1.36.0) [62] with
563 log2FoldChange ≥ 1 or ≤ -1 and adjusted *p*-value < 0.05 as cutoffs. Three biological
564 replicates of each sample were used to perform the transcriptome analyses.
565
566 **Plant experiments**

Strains selected for *in planta* assays were pre-cultured in 1/2 TSB at 25°C for 2-3 days until cloudy. On the day of inoculation, the bacterial culture was subcultured at a 1:3 ratio for an additional 5 hours. A 500 µL aliquot of bacterial culture was centrifuged at 6,500 × g for 2 min. After washing twice with 1 × PBS buffer, the bacterial pellets were resuspended in 1×PBS buffer and adjusted to an OD_{600} of 0.01. A 100 µL aliquot of bacterial suspension was then spread on half-strength Murashige and Skoog (MS) (Sigma-Aldrich, USA) plates supplemented with or without 100 nM IAA.

Arabidopsis seeds were surface-sterilized with 75% ethanol for 1 min, 20% bleach for 15 min, and rinsed 5 times with sterile distilled water. Seeds were sown evenly on 1/2 MS plates with 0.5% agar and 3% sucrose. After 2 days of stratification at 4°C in the dark, seeds were vertically grown in a growth chamber under a 16-h dark/8-h light regime at 22°C for 7 days. Ten seedlings were transferred to the prepared half-strength MS plates containing IAA and IAA-degrading bacteria. The initial position of the root tip was labeled, and after an additional 7 days of growth, the final position of the root tip was labeled again. Pictures of the plates were captured with a camera (Nikon, Japan), and the elongation of the primary root was measured using ImageJ [63].

Fluorescence microscopy

GFP fluorescence in the roots of *DR5::GFP* transgenic lines was visualized using a Ti2-E fluorescence microscope (Nikon, Japan) at 1 and 3 days after inoculation, respectively. The experiment was performed in two independent replicates.

592 **Measurement of bacteria root colonization**

593 Colony-forming units (CFUs) were counted as previously described with minor
594 modifications [64]. Briefly, after 7 days of inoculation, roots were separated from
595 shoots using a sterile scalpel, taking care to avoid contamination between different
596 bacterial treatments. Two roots were placed in pre-weighed sterile tubes containing
597 metal beads, and the tubes were weighed again to obtain the fresh weight of the roots.
598 Root samples were then homogenized using a TissueLyzer (Shanghai Cebo, China)
599 at 30 Hz for 30 seconds. A 500 µL aliquot of 1 × PBS buffer was added to the tube,
600 and the samples were serially diluted in a sterile 96-well plate. A 5 µL sample was
601 dropped onto a 1/2 TSB plate, and the plate was flipped sideways to allow the liquid
602 to flow evenly. Finally, the plates were placed at 25°C for two days until single
603 colonies appeared. The colonization ability of each strain on the root was calculated
604 according to the CFU count.

605

606 **ACKNOWLEDGEMENTS**

607 We gratefully acknowledge Prof. Paul Schulze-Lefert for sharing Arabidopsis
608 associated microbes. We gratefully acknowledge Prof. Xugang Li for providing
609 Arabidopsis auxin reporter transgenic line *DR5::GFP*.
610 The authors acknowledge the financial support from the National Natural Science
611 Foundation of China (No.32061143023), Guangdong Basic and Applied Basic
612 Research Foundation (No.2023A1515012006), Platform funding for Guangdong
613 Provincial Enterprise Key Laboratory of Seed and Seedling Health Management
614 Technology (2021B1212050011), Guizhou Provincial Basic Research Program
615 (Natural Science)-ZK[2023]-099, the Program of Introducing Talent to Chinese
616 Universities (111 Program, D20023), the Frontiers Science Center for Asymmetric

Synthesis and Medicinal Molecules, Department of Education, Guizhou Province [Qianjiaohe KY (2020)004].

AUTHOR CONTRIBUTION

LD and MXC designed and supervised the project. LXW and YL conducted the experiments. HRN, WLZ and HBL performed the bioinformatics analysis. HMS and WXL isolated the rice-associated microbes. HY provided the rice root samples. LXW and YL wrote the manuscript. LD, MXC, YB, HY, ACH, JF, TS and YGL reviewed and edited the manuscript. All authors approved the final manuscript.

AVAILABILITY OF DATA AND MATERIALS

The RNA-Seq data and Whole genome sequences of rice-associated isolates generated in this study were deposited to the European Nucleotide Archive (ENA) under the project accession PRJEB70882.

DECLARATIONS

Ethics approval and consent to participate

Not applicable.

CONSENT FOR PUBLICATION

Not applicable.

DECLARATION OF INTERESTS

The authors declare no competing interests.

643 # REFERENCE

644

645 1. Vanneste, S., and Friml, J. (2009). Auxin: a trigger for change in plant development.
646 Cell *136*, 1005-1016.
647 2. Zhao, Y. (2010). Auxin biosynthesis and its role in plant development. Annu Rev Plant
648 Biol *61*, 49-64.
649 3. Woodward, A.W., and Bartel, B. (2005). Auxin: regulation, action, and interaction.
650 Ann Bot *95*, 707-735.
651 4. Ross, J.J., O'Neill, D.P., Wolbang, C.M., Symons, G.M., and Reid, J.B. (2001).
652 Auxin-Gibberellin Interactions and Their Role in Plant Growth. Journal of Plant
653 Growth Regulation *20*, 346-353.
654 5. Ljung, K., Bhalerao, R.P., and Sandberg, G. (2001). Sites and homeostatic control of
655 auxin biosynthesis in Arabidopsis during vegetative growth. Plant J *28*, 465-474.
656 6. Petersson, S.V., Johansson, A.I., Kowalczyk, M., Makoveychuk, A., Wang, J.Y., Moritz,
657 T., Grebe, M., Benfey, P.N., Sandberg, G., and Ljung, K. (2009). An auxin gradient and
658 maximum in the Arabidopsis root apex shown by high-resolution cell-specific analysis
659 of IAA distribution and synthesis. Plant Cell *21*, 1659-1668.
660 7. Lopes, L.D., Futrell, S.L., Bergmeyer, E., Hao, J., and Schachtman, D.P. (2023). Root
661 exudate concentrations of indole-3-acetic acid (IAA) and abscisic acid (ABA) affect
662 maize rhizobacterial communities at specific developmental stages. FEMS Microbiol
663 Ecol *99*.
664 8. Lopez-Guerrero, M.G., Wang, P., Phares, F., Schachtman, D.P., Alvarez, S., and van
665 Dijk, K. (2022). A glass bead semi-hydroponic system for intact maize root exudate
666 analysis and phenotyping. Plant Methods *18*, 25.
667 9. Badri, D.V., and Vivanco, J.M. (2009). Regulation and function of root exudates. Plant
668 Cell Environ *32*, 666-681.
669 10. Trivedi, P., Leach, J.E., Tringe, S.G., Sa, T., and Singh, B.K. (2020). Plant-microbiome
670 interactions: from community assembly to plant health. Nat Rev Microbiol *18*,
671 607-621.
672 11. Lebeis, S.L., Paredes, S.H., Lundberg, D.S., Breakfield, N., Gehring, J., McDonald, M.,
673 Malfatti, S., Glavina del Rio, T., Jones, C.D., Tringe, S.G., et al. (2015). PLANT
674 MICROBIOME. Salicylic acid modulates colonization of the root microbiome by
675 specific bacterial taxa. Science *349*, 860-864.
676 12. Eichmann, R., Richards, L., and Schäfer, P. (2021). Hormones as go-betweens in plant
677 microbiome assembly. Plant J *105*, 518-541.
678 13. Wang, L., Chen, M., Lam, P.Y., Dini-Andreote, F., Dai, L., and Wei, Z. (2022).
679 Multifaceted roles of flavonoids mediating plant-microbe interactions. Microbiome
680 *10*, 233.
681 14. Tzipilevich, E., Russ, D., Dangl, J.L., and Benfey, P.N. (2021). Plant immune system
682 activation is necessary for efficient root colonization by auxin-secreting beneficial
683 bacteria. Cell Host Microbe *29*, 1507-1520.e1504.
684 15. Patten, C.L., and Glick, B.R. (1996). Bacterial biosynthesis of indole-3-acetic acid. Can
685 J Microbiol *42*, 207-220.

16. Leveau, J.H., and Gerards, S. (2008). Discovery of a bacterial gene cluster for catabolism of the plant hormone indole 3-acetic acid. FEMS Microbiol Ecol *65*, 238-250.
17. Lin, G.H., Chen, H.P., Huang, J.H., Liu, T.T., Lin, T.K., Wang, S.J., Tseng, C.H., and Shu, H.Y. (2012). Identification and characterization of an indigo-producing oxygenase involved in indole 3-acetic acid utilization by Acinetobacter baumannii. Antonie Van Leeuwenhoek *101*, 881-890.
18. Scott, J.C., Greenhut, I.V., and Leveau, J.H. (2013). Functional characterization of the bacterial iac genes for degradation of the plant hormone indole-3-acetic acid. J Chem Ecol *39*, 942-951.
19. Shu, H.Y., Lin, L.C., Lin, T.K., Chen, H.P., Yang, H.H., Peng, K.C., and Lin, G.H. (2015). Transcriptional regulation of the iac locus from Acinetobacter baumannii by the phytohormone indole-3-acetic acid. Antonie Van Leeuwenhoek *107*, 1237-1247.
20. Donoso, R., Leiva-Novoa, P., Zúñiga, A., Timmermann, T., Recabarren-Gajardo, G., and González, B. (2017). Biochemical and Genetic Bases of Indole-3-Acetic Acid (Auxin Phytohormone) Degradation by the Plant-Growth-Promoting Rhizobacterium Paraburkholderia phytofirmans PsJN. Appl Environ Microbiol *83*.
21. Greenhut, I.V., Slezak, B.L., and Leveau, J.H.J. (2018). iac Gene Expression in the Indole-3-Acetic Acid-Degrading Soil Bacterium Enterobacter soli LF7. Appl Environ Microbiol *84*.
22. Sadauskas, M., Statkevičiūtė, R., Vaitekūnas, J., and Meškys, R. (2020). Bioconversion of Biologically Active Indole Derivatives with Indole-3-Acetic Acid-Degrading Enzymes from Caballeronia glathei DSM50014. Biomolecules *10*.
23. Jensen, J.B., Egsgaard, H., Van Onckelen, H., and Jochimsen, B.U. (1995). Catabolism of indole-3-acetic acid and 4- and 5-chloroindole-3-acetic acid in Bradyrhizobium japonicum. J Bacteriol *177*, 5762-5766.
24. Conway, J.M., Walton, W.G., Salas-González, I., Law, T.F., Lindberg, C.A., Crook, L.E., Kosina, S.M., Fitzpatrick, C.R., Lietzan, A.D., Northen, T.R., et al. (2022). Diverse MarR bacterial regulators of auxin catabolism in the plant microbiome. Nat Microbiol *7*, 1817-1833.
25. Finkel, O.M., Salas-González, I., Castrillo, G., Conway, J.M., Law, T.F., Teixeira, P., Wilson, E.D., Fitzpatrick, C.R., Jones, C.D., and Dangl, J.L. (2020). A single bacterial genus maintains root growth in a complex microbiome. Nature *587*, 103-108.
26. Donati, A.J., Lee, H.I., Leveau, J.H., and Chang, W.S. (2013). Effects of indole-3-acetic acid on the transcriptional activities and stress tolerance of Bradyrhizobium japonicum. PLoS One *8*, e76559.
27. Nascimento, F.X., Glick, B.R., and Rossi, M.J. (2021). Multiple plant hormone catabolism activities: an adaptation to a plant-associated lifestyle by Achromobacter spp. Environ Microbiol Rep *13*, 533-539.
28. Deochand, D.K., and Grove, A. (2017). MarR family transcription factors: dynamic variations on a common scaffold. Crit Rev Biochem Mol Biol *52*, 595-613.
29. Gang, S., Sharma, S., Saraf, M., Buck, M., and Schumacher, J. (2019). Analysis of Indole-3-acetic Acid (IAA) Production in Klebsiellaby LC-MS/MS and the Salkowski Method. Bio Protoc *9*, e3230.
30. Perera, I.C., and Grove, A. (2010). Molecular mechanisms of ligand-mediated attenuation of DNA binding by MarR family transcriptional regulators. J Mol Cell Biol *2*, 243-254.

31. Jumper, J., Evans, R., Pritzel, A., Green, T., Figurnov, M., Ronneberger, O., Tunyasuvunakool, K., Bates, R., Žídek, A., Potapenko, A., et al. (2021). Highly accurate protein structure prediction with AlphaFold. Nature *596*, 583-589.
32. Zhang, Y., and Skolnick, J. (2005). TM-align: a protein structure alignment algorithm based on the TM-score. Nucleic Acids Res *33*, 2302-2309.
33. Xu, J., and Zhang, Y. (2010). How significant is a protein structure similarity with TM-score = 0.5? Bioinformatics *26*, 889-895.
34. He, D., Singh, S.K., Peng, L., Kaushal, R., Vílchez, J.I., Shao, C., Wu, X., Zheng, S., Morcillo, R.J.L., Paré, P.W., et al. (2022). Flavonoid-attracted Aeromonas sp. from the Arabidopsis root microbiome enhances plant dehydration resistance. Isme j *16*, 2622-2632.
35. Seitz, V.A., McGivern, B.B., Daly, R.A., Chaparro, J.M., Borton, M.A., Sheflin, A.M., Kresovich, S., Shields, L., Schipanski, M.E., Wrighton, K.C., et al. (2022). Variation in Root Exudate Composition Influences Soil Microbiome Membership and Function. Appl Environ Microbiol *88*, e0022622.
36. Bandla, A., Pavagadhi, S., Sridhar Sudarshan, A., Poh, M.C.H., and Swarup, S. (2020). 910 metagenome-assembled genomes from the phytobiomes of three urban-farmed leafy Asian greens. Sci Data *7*, 278.
37. Zhang, H., Wang, M., Wang, H., Chen, H., Cao, L., Zhong, Z., Lian, C., Zhou, L., and Li, C. (2022). Metagenome sequencing and 768 microbial genomes from cold seep in South China Sea. Sci Data *9*, 480.
38. Su, P., Wicaksono, W.A., Li, C., Michl, K., Berg, G., Wang, D., Xiao, Y., Huang, R., Kang, H., Zhang, D., et al. (2022). Recovery of metagenome-assembled genomes from the phyllosphere of 110 rice genotypes. Sci Data *9*, 254.
39. Xie, F., Jin, W., Si, H., Yuan, Y., Tao, Y., Liu, J., Wang, X., Yang, C., Li, Q., Yan, X., et al. (2021). An integrated gene catalog and over 10,000 metagenome-assembled genomes from the gastrointestinal microbiome of ruminants. Microbiome *9*, 137.
40. Bai, Y., Müller, D.B., Srinivas, G., Garrido-Oter, R., Potthoff, E., Rott, M., Dombrowski, N., Münch, P.C., Spaepen, S., Remus-Emsermann, M., et al. (2015). Functional overlap of the Arabidopsis leaf and root microbiota. Nature *528*, 364-369.
41. Wippel, K., Tao, K., Niu, Y., Zgadzaj, R., Kiel, N., Guan, R., Dahms, E., Zhang, P., Jensen, D.B., Logemann, E., et al. (2021). Host preference and invasiveness of commensal bacteria in the Lotus and Arabidopsis root microbiota. Nat Microbiol *6*, 1150-1162.
42. Nayfach, S., Roux, S., Seshadri, R., Udwary, D., Varghese, N., Schulz, F., Wu, D., Paez-Espino, D., Chen, I.M., Huntemann, M., et al. (2021). A genomic catalog of Earth's microbiomes. Nat Biotechnol *39*, 499-509.
43. Coelho, L.P., Alves, R., del Río, Á.R., Myers, P.N., Cantalapiedra, C.P., Giner-Lamia, J., Schmidt, T.S., Mende, D.R., Orakov, A., Letunic, I., et al. (2022). Towards the biogeography of prokaryotic genes. Nature *601*, 252-256.
44. Betoudji, F., Abd El Rahman, T., Miller, M.J., Ghosh, M., Jacques, M., Bouarab, K., and Malouin, F. (2020). A Siderophore Analog of Fimsbactin from Acinetobacter Hinders Growth of the Phytopathogen Pseudomonas syringae and Induces Systemic Priming of Immunity in Arabidopsis thaliana. Pathogens *9*.
45. Xie, J., Yan, Z., Wang, G., Xue, W., Li, C., Chen, X., and Chen, D. (2020). A Bacterium Isolated From Soil in a Karst Rocky Desertification Region Has Efficient Phosphate-Solubilizing and Plant Growth-Promoting Ability. Front Microbiol *11*, 625450.

46. Lin, H.R., Shu, H.Y., and Lin, G.H. (2018). Biological roles of indole-3-acetic acid in Acinetobacter baumannii. Microbiol Res *216*, 30-39.
47. Li, D., Liu, R., Wang, M., Peng, R., Fu, S., Fu, A., Le, J., Yao, Q., Yuan, T., Chi, H., et al. (2022). 3β-Hydroxysteroid dehydrogenase expressed by gut microbes degrades testosterone and is linked to depression in males. Cell Host Microbe *30*, 329-339.e325.
48. Belimov, A.A., Dodd, I.C., Safronova, V.I., Dumova, V.A., Shaposhnikov, A.I., Ladatko, A.G., and Davies, W.J. (2014). Abscisic acid metabolizing rhizobacteria decrease ABA concentrations in planta and alter plant growth. Plant Physiology and Biochemistry *74*, 84-91.
49. Chen, S., Zhou, Y., Chen, Y., and Gu, J. (2018). fastp: an ultra-fast all-in-one FASTQ preprocessor. Bioinformatics *34*, i884-i890.
50. Wick, R.R., Judd, L.M., Gorrie, C.L., and Holt, K.E. (2017). Unicycler: resolving bacterial genome assemblies from short and long sequencing reads. PLoS computational biology *13*, e1005595.
51. Parks, D.H., Imelfort, M., Skennerton, C.T., Hugenholtz, P., and Tyson, G.W. (2015). CheckM: assessing the quality of microbial genomes recovered from isolates, single cells, and metagenomes. Genome research *25*, 1043-1055.
52. Seemann, T. (2014). Prokka: rapid prokaryotic genome annotation. Bioinformatics *30*, 2068-2069.
53. Chaumeil, P.-A., Mussig, A.J., Hugenholtz, P., and Parks, D.H. (2020). GTDB-Tk: a toolkit to classify genomes with the Genome Taxonomy Database. (Oxford University Press).
54. Zhou, C., Xu, Q., He, S., Ye, W., Cao, R., Wang, P., Ling, Y., Yan, X., Wang, Q., and Zhang, G. (2020). GTDB: an integrated resource for glycosyltransferase sequences and annotations. Database *2020*.
55. Edgar, R.C. (2022). Muscle5: High-accuracy alignment ensembles enable unbiased assessments of sequence homology and phylogeny. Nat Commun *13*, 6968.
56. Kumar, S., Stecher, G., Li, M., Knyaz, C., and Tamura, K. (2018). MEGA X: Molecular Evolutionary Genetics Analysis across Computing Platforms. Mol Biol Evol *35*, 1547-1549.
57. Letunic, I., and Bork, P. (2019). Interactive Tree Of Life (iTOL) v4: recent updates and new developments. Nucleic Acids Res *47*, W256-w259.
58. Buchfink, B., Xie, C., and Huson, D.H. (2015). Fast and sensitive protein alignment using DIAMOND. Nat Methods *12*, 59-60.
59. Ewels, P.A., Peltzer, A., Fillinger, S., Patel, H., Alneberg, J., Wilm, A., Garcia, M.U., Di Tommaso, P., and Nahnsen, S. (2020). The nf-core framework for community-curated bioinformatics pipelines. Nat Biotechnol *38*, 276-278.
60. Dobin, A., Davis, C.A., Schlesinger, F., Drenkow, J., Zaleski, C., Jha, S., Batut, P., Chaisson, M., and Gingeras, T.R. (2013). STAR: ultrafast universal RNA-seq aligner. Bioinformatics *29*, 15-21.
61. Patro, R., Duggal, G., Love, M.I., Irizarry, R.A., and Kingsford, C. (2017). Salmon provides fast and bias-aware quantification of transcript expression. Nat Methods *14*, 417-419.
62. Love, M.I., Huber, W., and Anders, S. (2014). Moderated estimation of fold change and dispersion for RNA-seq data with DESeq2. Genome Biol *15*, 550.

826 63. Schneider, C.A., Rasband, W.S., and Eliceiri, K.W. (2012). NIH Image to ImageJ: 25
827 years of image analysis. Nat Methods *9*, 671-675.
828 64. Ma, K.W., Ordon, J., and Schulze-Lefert, P. (2022). Gnotobiotic Plant Systems for
829 Reconstitution and Functional Studies of the Root Microbiota. Curr Protoc *2*, e362.
830 65. Xu, S., Chen, M., Feng, T., Zhan, L., Zhou, L., and Yu, G. (2021). Use ggbreak to
831 effectively utilize plotting space to deal with large datasets and outliers. Frontiers in
832 Genetics *12*, 2122.
833

834

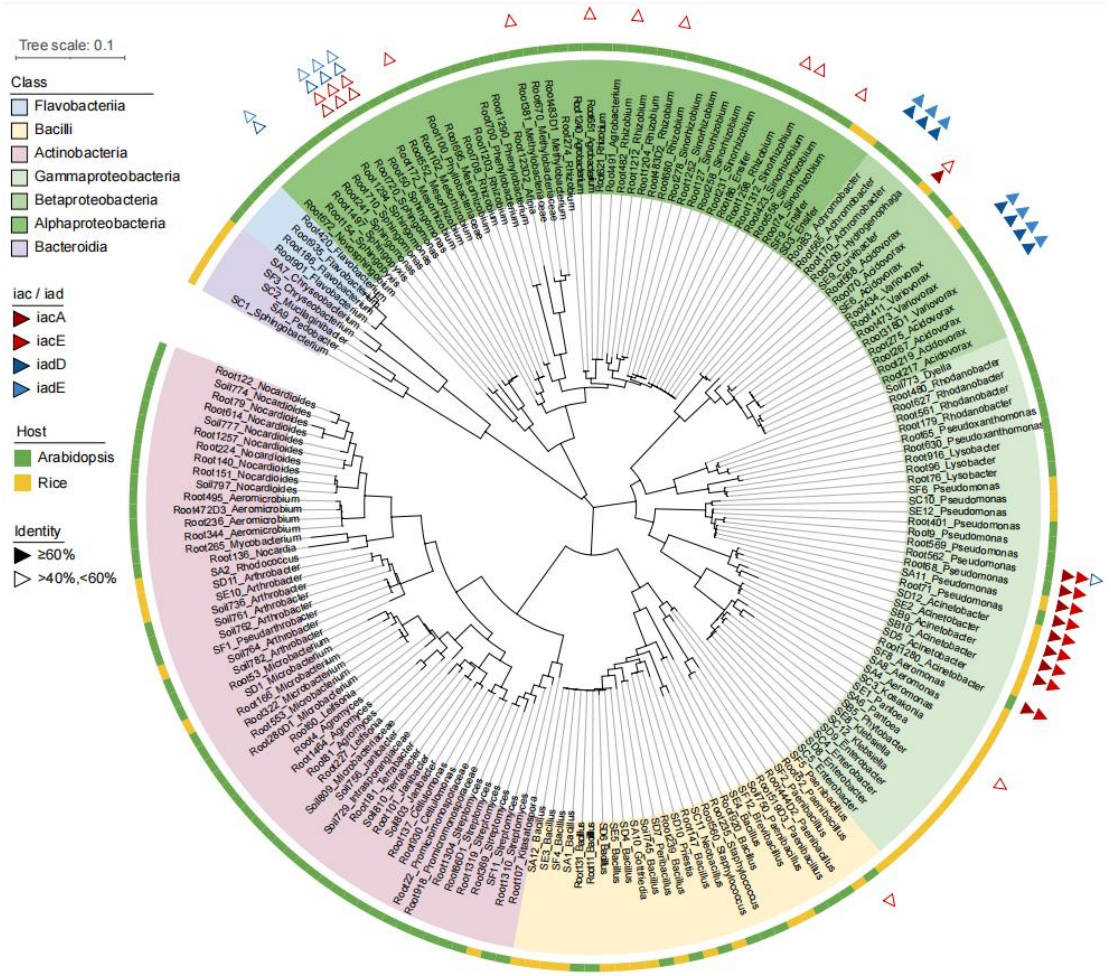

Figure 1. Bacterial strains isolated from Arabidopsis and rice rhizosphere are annotated for genes related to IAA degradation. The 16S rRNA-based phylogenetic tree of the 189 strains was generated with MEGA-X and visualized with iTOL. Strains annotated to have iacA/E or iadD/E (over 40% identity and 60% coverage with template amino acid sequences, see Methods) were labeled with triangles.

848

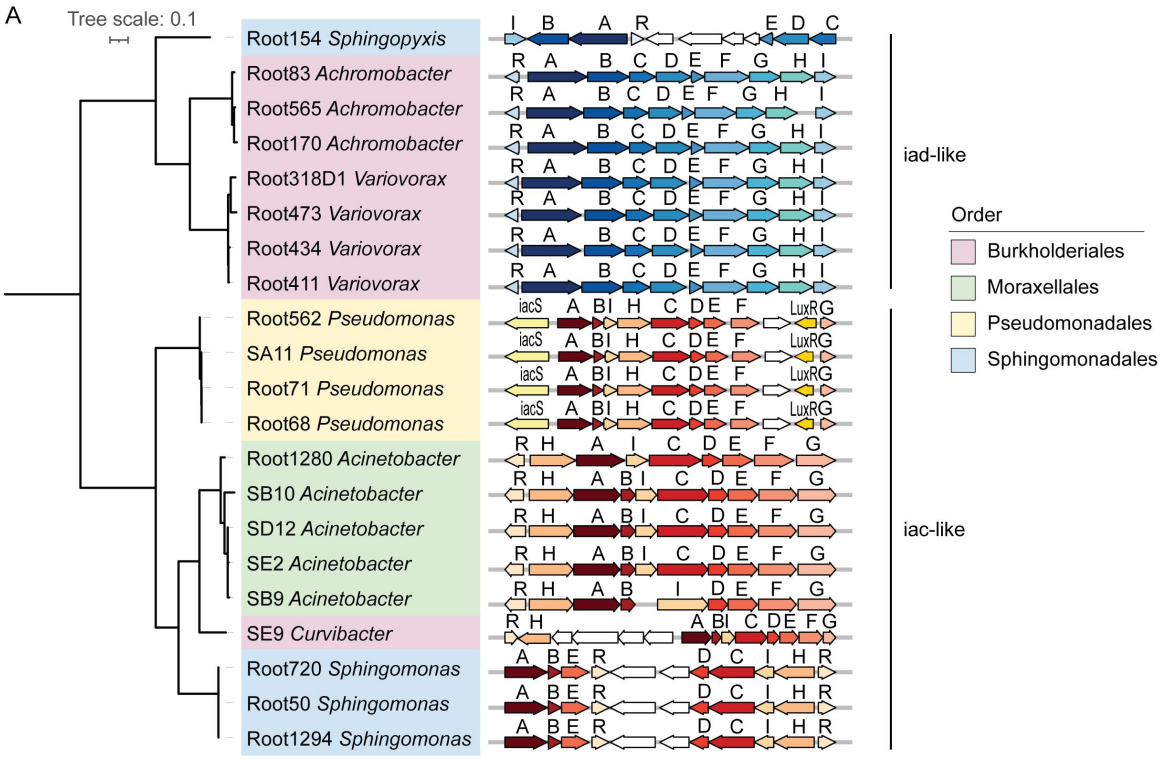

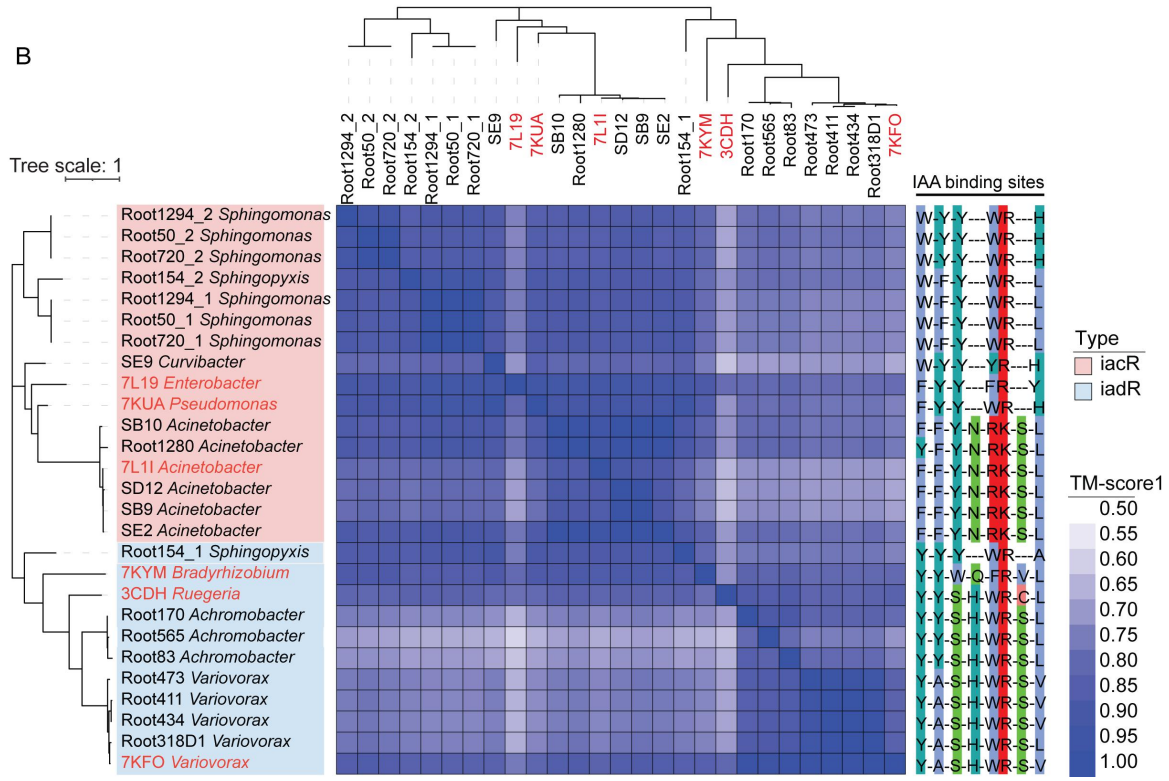

849

850

851

852 **Figure 2**. **Identification of gene clusters related to IAA degradation and the**
853 **corresponding MarR family regulators.** (A), Organization of *iac* and *iad* gene
854 clusters in 21 IAA-degrading strains. Phylogenetic tree constructed using the
855 concatenated iacA and iacE or iadD and iadE amino acid sequences. Gene
856 transcription directions are indicated by arrows. Letters above the red or blue arrows
857 indicate function genes in the cluster with high protein sequence identity compared to
858 the templates. White arrows indicate genes in this cluster with unknown function. (B),
859 Protein structures of iacR or iadR (all belong to MarR family) are highly conserved
860 among IAA-degrading strains. Heatmap of the protein structural similarity among 27
861 MarR family proteins displayed the TM1 score. iacR or iadR retrieved from 17
862 IAA-degrading strains in this study and 6 reference proteins which protein structures
863 and IAA binding sites have been identified. The phylogenetic tree was constructed
864 using the iacR or iadR amino acid sequences. The IAA binding sites of MarR were
865 conservatively distributed in iacR or iadR. Six MarR templates used in this analysis
866 (labeled in red) are 7L1I *Acinetobacter baumannii*, 7KUA *Pseudomonas putida*, 7L19
867 *Enterobacter soli* ATCC BAA-2102, 7KYM *Bradyrhizobium japonicum*, 3CDH
868 *Ruegeria pomeroyi* DSS-3, 7KFO *Variovorax paradoxus* CL14.
869
870

871

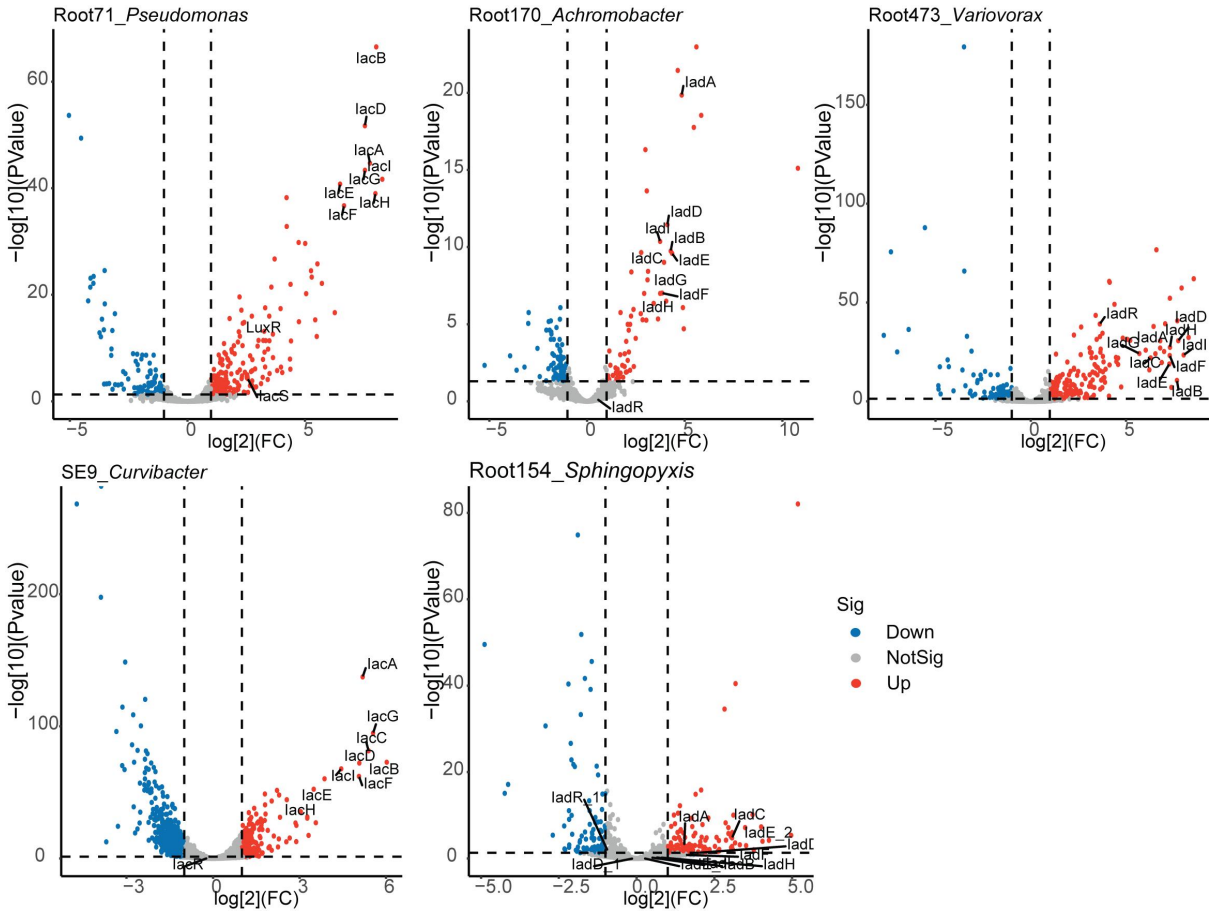

872

873 **Figure 3. RNA-seq reveals that the transcription of the iac-like or iad-like gene**
874 **cluster is induced by IAA.** The 5 selected strains for RNA-seq analysis were
875 cultured with M9 medium supplemented with either IAA or glucose as the sole carbon
876 source. The deferential expression genes between IAA and Glucose treatments were
877 analyzed. Significantly up-regulated or down-regulated genes were identified with
878 $\log_2^{\text{FoldChange}} \geq 1$ or ≤ -1 and adjusted *p*-value < 0.05 as cutoffs. Three individual colony
879 of each strain were used to perform the transcriptome analyses.

880

881

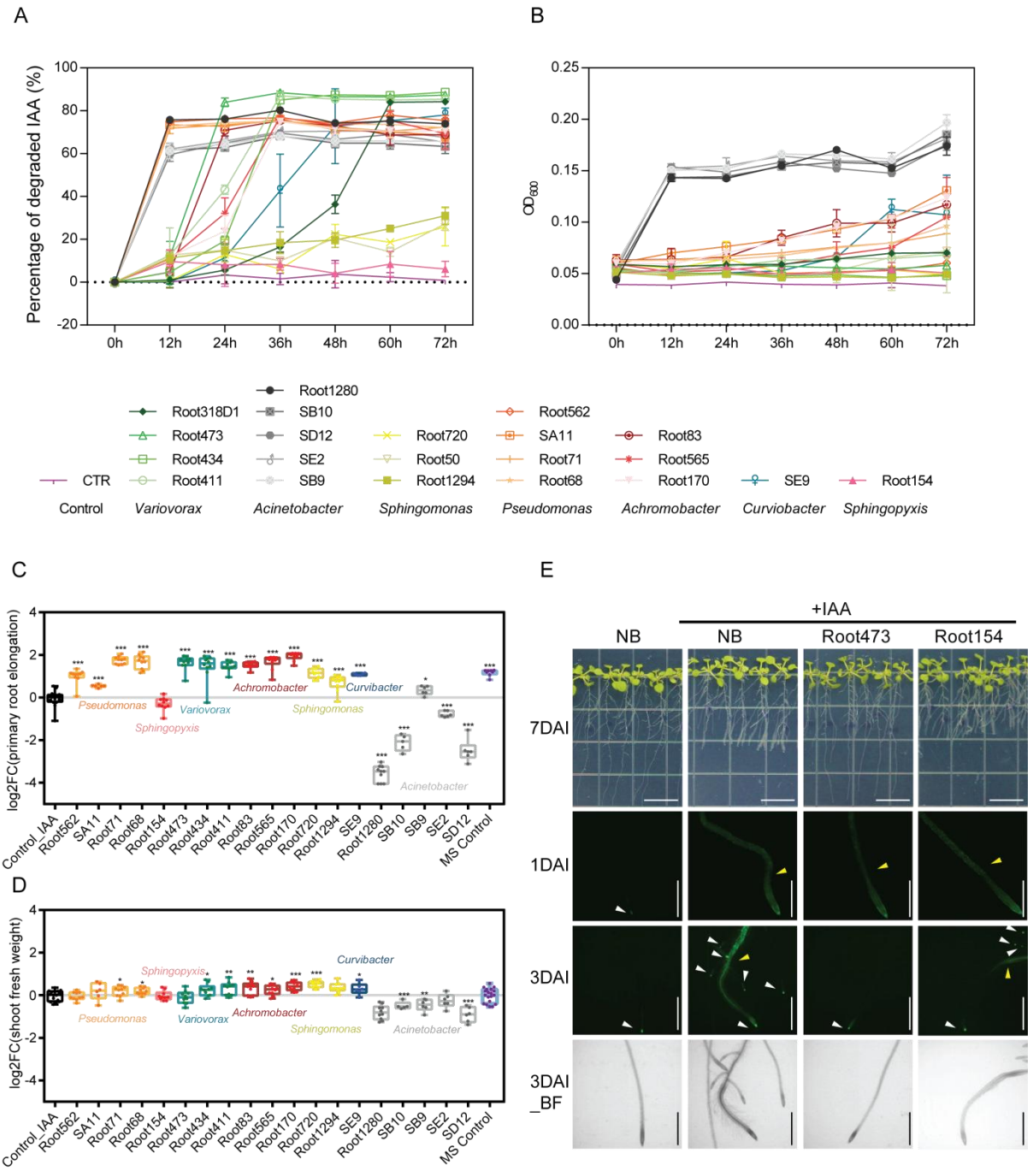

Figure 4. IAA-degrading strains can utilize IAA and suppress the IAA-induced root growth inhibition. (A), IAA consumed by IAA degraders *in vitro* and (B) their growth as measured by OD_{600} in M9 minimal medium supplemented with IAA as the sole carbon source (n=4). (C), Except for strains from genus of *Sphingopyxis* and *Acinetobacter*, IAA-induced root growth inhibition was suppressed by IAA-degrading

889 strains. Boxplot middle line, median log2 fold change of primary root elongation (vs
890 Control_IAA); box edges, 25th and 75th percentiles; whiskers, 1.5× the interquartile
891 range. Left to right n = 16, 10, 6, 10, 10, 10, 10, 10, 10, 10, 10, 10, 10, 10, 6, 10, 5, 6,
892 6, and 8 biological replicates. (D), Apart from *Acinetobacter*, strains inoculation have
893 no negative effects on shoot fresh weight. Boxplot middle line, median log2 fold
894 change of shoot fresh weight (vs Control_IAA); box edges, 25th and 75th percentiles;
895 whiskers, 1.5× the interquartile range. Left to right n = 17, 10, 10, 6, 10, 10, 10, 10, 10,
896 10, 10, 10, 10, 10, 10, 10, 7, 9, 9, and 19 biological replicates. (E), Images of
897 representative Col-0 seedlings grown axenically (NB) or with IAA-degrading strain
898 inoculation. Upper panes show the representative images of seedlings grown on 1/2
899 MS agar plate supplemented with 100nM IAA at 7 days after inoculation with or
900 without strain. Bar = 1.4cm. The other planes show the representative primary root
901 images of *DR5::GFP* plants after inoculated with strain for 1 and 3 days. Bar = 1mm.
902 Write arrows show the GFP signal on root tips. Yellow arrows show the GFP signals
903 on root which were induced by exogenous IAA. BF, bright field. Significant differences
904 compared with control group were determined using Student's *t*-test: **P*<0.05,
905 ***P*<0.01, ****P*<0.001.
906
907

908

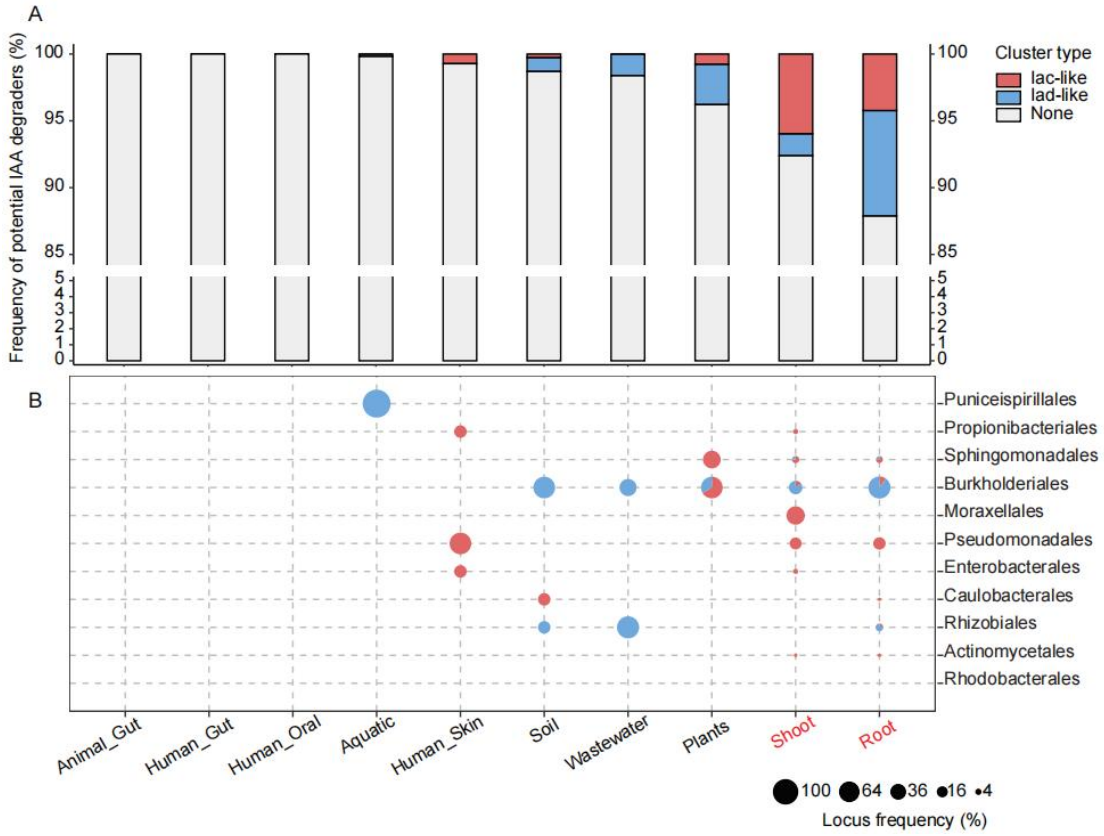

909

910 **Figure 5. The distribution of IAA-degrading bacterial strains across various**
911 **habitats.** (A), The frequency of potential IAA degraders whose genome contains iacA
912 and iacE or iadD and iadE in different habitats. IAA degradation types were labeled
913 with red or blue color. Ggbreak was applied in this analysis [65]. (B), IAA degradation
914 types are varied at bacterial order level. In total, 11,586 high quality MAGs and
915 isolates were analyzed in this study. Samples containing isolates were highlighted
916 with red color. All MAGs were ≥90% complete, were ≤5% contaminated and had a
917 quality score (completeness - 5 × contamination) of ≥65.

918
919